



Improving Na-O₂ batteries with redox mediators

James T. Frith^a, Imanol Landa-Medrano^{b,c}, Idoia Ruiz de Larramendi^b, Teófilo Rojo^{b,d}, John R. Owen^a, Nuria Garcia-Araez^{a,*}

Received 00th January 20xx,
Accepted 00th January 20xx

DOI: 10.1039/x0xx00000x

www.rsc.org/

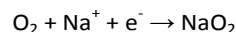
A new route to enhance the performance of Na-O₂ cells is demonstrated. Redox mediators (such as ethyl viologen) are shown to facilitate the discharge reaction, producing an increased capacity (due to suppressed electrode passivation), higher discharge potential (due to faster kinetics) and stable cycling.

Na-O₂ batteries are among the most promising post Li-ion candidates, due to their high theoretical specific energy (1108 Wh kg⁻¹ based on the reduction of O₂ to NaO₂), low cost and reversible electrochemical performance.^{1–4} Remarkable advances have been made in recent years, especially in the elucidation of the reaction mechanism.^{5–10} Hartmann et al.¹¹ were the first group to discuss the possibility of two competing reaction pathways for the formation of NaO₂ discharge particles: superoxide could be stabilized in the electrolyte and precipitate after saturation (solution mechanism), or the direct formation and growth of NaO₂ could take place at the electrode surface (surface mechanism). The same group demonstrated later that the solution mechanism was the main reaction pathway due to the stability and solubility of sodium superoxide in the electrolyte.¹² In fact, Xia et al.¹³ evidenced that trace amounts of water could facilitate this stabilization, as protons in the electrolyte acted as phase transfer catalysts during the oxygen reduction reaction, ORR. Recently, Lutz et al.¹⁴ found that the kinetics of desolvation of soluble NaO₂ species, which is a critical step before nucleation and growth of NaO₂ particles, is a key factor governing the capacity of the cell. Slow desolvation leads to slow precipitation, and thus, super-saturation of NaO₂ near the electrode surface, producing fast precipitation of NaO₂ at the electrode surface,

leading to electrode passivation and low capacities. Incomplete utilization of the porous carbon electrode and inhomogeneous distribution of NaO₂ deposits have also been demonstrated.^{15–17}

The strategies employed for enhancing the performance of Na-O₂ batteries have been so far limited to exploring the effect of the electrolyte and the oxygen electrode structure and composition.^{18–20} Here, we demonstrate a new route to enhance the performance of Na-O₂ batteries: the introduction of homogenous catalysis (also called redox mediators). On the example of ethyl viologen,^{21,22} it is shown that the reaction mechanism is transformed by redox mediators, since the ORR takes place via the chemical reaction of oxygen with the reduced form of the redox mediator. As a result, a lower discharge overpotential and an increased capacity are observed. Two recent studies have explored the use of redox mediators to facilitate charging of Na-O₂ cells,^{23,24} but this is the first work demonstrating an enhancement of the discharge performance upon addition of redox mediators. Redox mediators for discharge have been used in Li-O₂ cells to facilitate the formation of Li₂O₂ and suppress superoxide species,^{21,22} but that effect might not be advantageous in Na-O₂ cells where NaO₂ formation has been shown to lead to better rechargeability than peroxide species.^{3,25}

Figure 1 shows the effect of ethyl viologen on the discharge profile of Na-O₂ cells and the evaluation of the amount of O₂ consumed from the change in the O₂ pressure during the discharge process. In all cases, the amount of O₂ consumed correlates well with a one-electron process where one electron is consumed per oxygen molecule:²⁶



^a Department of Chemistry, University of Southampton, SO17 1BJ, Southampton, UK.

^b Departamento de Química Inorgánica, Facultad de Ciencia y Tecnología, Universidad del País Vasco (UPV/EHU) Barrio Sarriena s/n, 48940 Leioa - Bizkaia, Spain.

^c BCMaterials, Parque Científico y Tecnológico de Bizkaia, 48160 Derio - Bizkaia, Spain.

^d CIC EnergiGUNE, Albert Einstein 48, 0150, Miñano, Spain

* n.garcia-araez@soton.ac.uk

Electronic Supplementary Information (ESI) available: Experimental details and additional electrochemical experiments. See DOI: 10.1039/x0xx00000x

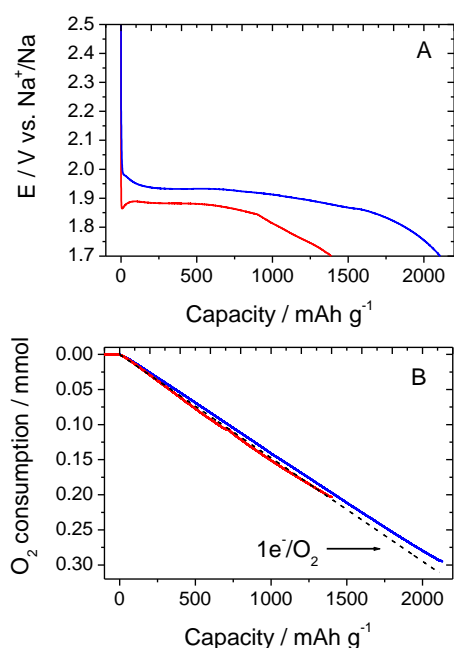
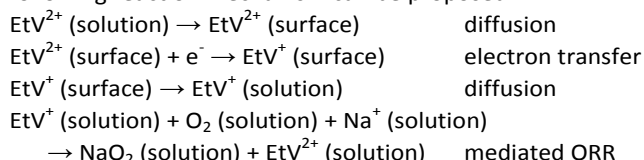


Figure 1. Galvanostatic discharge of Na-O₂ cells at 200 mA g⁻¹ (A) and corresponding change in the number of moles of oxygen as evaluated by pressure change measurements (B), for cells containing 250 mM NaOTf in diglyme with (-) and without (-) 10 mM EtV(OTf)₂. The dashed line in Figure 1B shows the expected behaviour for a 1e⁻/O₂ reaction. Cells were assembled with a sodium conductive membrane to prevent mass transport of viologen to the sodium electrode (see ESI for details).

It is observed that the capacity increases dramatically upon addition of ethyl viologen (by 50% under the present conditions), which we attribute to the fact that ethyl viologen facilitates the reduction of oxygen in solution, promoting the aforementioned solution-mechanism and avoiding the fast saturation of NaO₂ in the electrolyte nearby the oxygen electrode. This hinders the passivation of the electrode and the discharge capacity is therefore increased, as the end of discharge of Na-O₂ batteries is associated to the blockage of the electrode surface by discharge products.^{7,23,27} Notably, the increased capacity is also observed on charging (Figure S1) and no additional plateaus are observed, demonstrating that the additional capacity in presence of the redox mediator corresponds to the formation of reversible NaO₂. In addition, Figure 1 shows that the discharge potential increases by ca. 0.1 V upon addition of ethyl viologen, attributable to more facile kinetics of the mediated oxygen reduction reaction. The following reaction mechanism can be proposed:



The formation of NaO₂ as the main discharge product, with and without viologen, is confirmed by the ex-situ characterization of the discharged electrodes by XRD and Raman, as shown in Figures 2A and 2B, respectively.

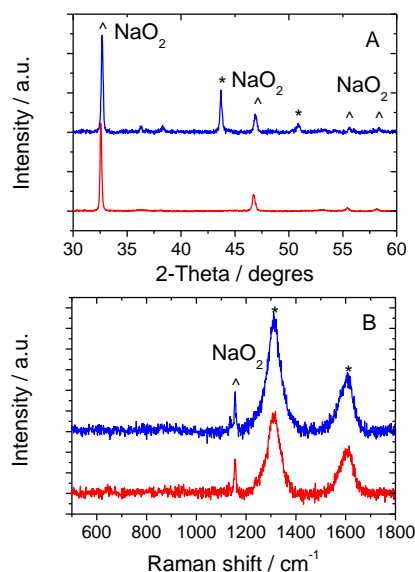


Figure 2. Ex-situ analysis of discharged electrodes: A) XRD data, where (^) denotes peaks due to NaO₂,⁴ and (*) denotes peaks due to stainless steel mesh. B) Raman spectra, where (^) denotes peaks due to NaO₂,^{28,29} and (*) denotes peaks due to carbon. Electrochemical conditions as in figure 1, where electrodes have been discharged in cells with (-) and without (-) 10 mM EtV(OTf)₂.

The mediation of the oxygen reduction reaction by EtV⁺ is proposed in view of the comparison of the discharge profile in Ar and in O₂ for viologen-containing cells (Figure 3). The discharge in Ar shows two characteristic potential plateaus corresponding to the reduction of EtV²⁺ to EtV⁺ at 2.3 V, and that of EtV⁺ to EtV⁰ at 1.9 V vs. Na⁺/Na. The discharge in O₂ takes place at potentials close to the EtV²⁺ to EtV⁺ conversion, indicating that the reduction of oxygen is initiated by the reduction of EtV²⁺ to EtV⁺, as proposed in the reaction mechanism above. The discharge potential in O₂ is slightly lower than the EtV²⁺/EtV⁺ potential plateau in Ar, fact that could be ascribed to an increased IR drop due to deposition of small amounts of NaO₂ on the electrode surface or the separator. On the other hand, the reduction of EtV⁺ to EtV⁰ takes place at much lower potentials than the ORR, demonstrating that formation of EtV⁰ is not required to mediate the reduction of oxygen. Cyclic voltammetry measurements at a flat glassy carbon electrode (Figure S2) also evidence the catalytic activity of ethyl viologen, in terms of increasing the oxygen reduction current. However, it is difficult to discern the nature of the mediator species (EtV⁺ or EtV⁰) from the voltammetric measurements due to overlapping of the different processes.

UV-vis titration experiments were performed in order to prove the reaction between O₂ and EtV⁺. Aliquots of O₂-saturated solution were added to an EtV⁺ solution (Figure 4), in such a way that each aliquot contained an amount of O₂ equal to 20% of the moles of EtV⁺. The UV-vis spectra show a decrease in the EtV⁺ absorbance peaks and an increase in the EtV²⁺ peaks that agree quantitatively with the stoichiometry of the mechanism above proposed, where one EtV⁺ reacts with one O₂ molecule to form one EtV²⁺ (Figure S7).

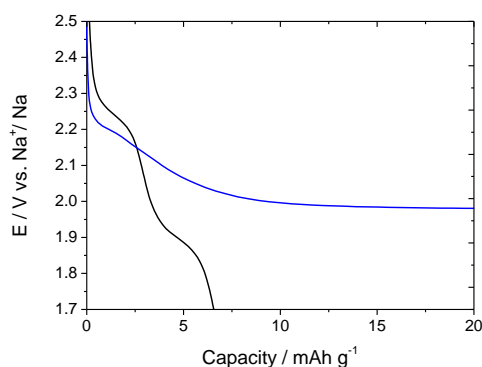


Figure 3. Galvanostatic discharge of cells containing 10 mM EtV(OTf)₂ + 250 mM NaOTf in diglyme in Ar (-) and O₂ (-). Electrochemical conditions as in figure 1.

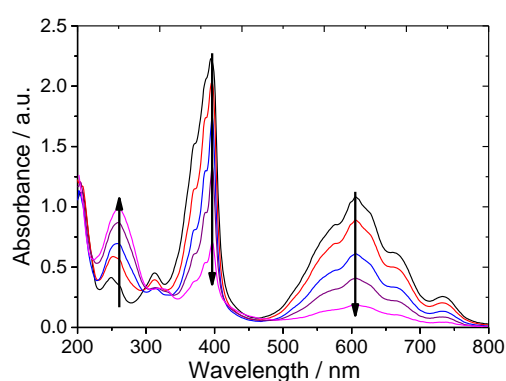


Figure 4. UV-Vis spectra recorded during the titration of EtV⁺ by O₂. (-) EtV⁺ solution, after addition of (-) 1st aliquot (-) 2nd aliquot (-) 3rd aliquot (-) 4th aliquot. The number of moles of oxygen in each aliquot was equal to 1/5th of the number of moles of EtV⁺ initially present in the solution.

Since, in the presence of viologen, the reduction of oxygen takes place in solution rather than on the electrode surface, the extent of electrode pore clogging and electrode passivation decreases upon addition of viologen, as shown in the SEM images of the discharged electrodes (Figure 5). Higher amounts of relatively big NaO₂ crystals are observed on electrodes cycled in the presence of ethyl viologen, which are formed via the viologen-facilitated solution-based reduction of oxygen (Figure 5B). On the contrary, in the absence of viologen, there is a competition between the solution-based formation of NaO₂ and the direct electrochemical reduction of oxygen to form NaO₂ deposits on the electrode surface. The latter pathway would produce a thin, passivating NaO₂ deposit on top of the electrode surface, resulting in an early end of discharge and hence, a smaller discharge capacity (see the sketch in Figure 6). This thin passivating layer is difficult to detect by ex-situ SEM measurements, but clearly fewer NaO₂ particles are observed in electrodes discharged in the absence of ethyl viologen (Figure 5A). The results demonstrate that the reaction pathway is changed in the presence of ethyl viologen, and pore clogging and electrode passivation is mitigated because NaO₂ formation takes place further away from the electrode surface (see the sketch in Figure 6).

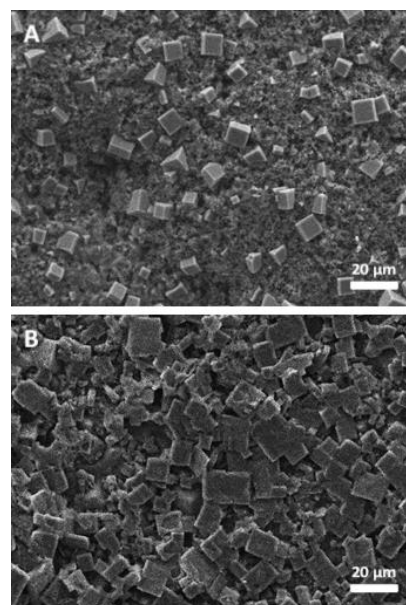


Figure 5. SEM images of electrodes discharged in cells without (A) and with (B) 10 mM EtV(OTf)₂. Electrochemical conditions as in figure 1.

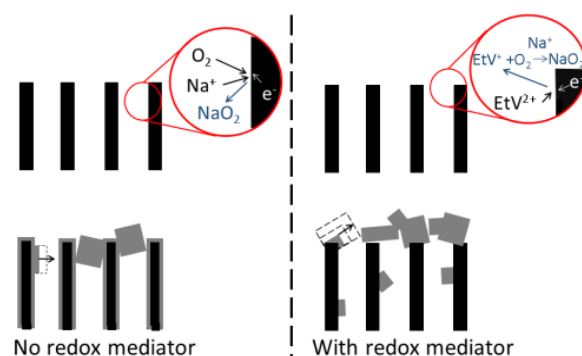


Figure 6. Diagram of sodium superoxide formation via an unmediated and mediated reaction pathway (black: carbon, NaO₂: grey).

The improved capacity achieved upon addition of ethyl viologen is sustained for many cycles, for both charge and discharge (see Figure S1). The coulombic efficiencies are the same in the presence and absence of viologen (ca 90% in the first cycle and ca 93% in subsequent ones). It has been shown that the mechanism of the charge reaction in Na-O₂ cells involves (i) direct oxidation of thin NaO₂ deposits producing O₂ and unblocked carbon areas, and (ii) dissolution of thicker NaO₂ deposits into soluble NaO₂ species that are oxidized on the free carbon areas.^{5,10,30} The rechargeability of the cell is compromised when products other than NaO₂ are formed (e.g. NaOH or Na₂CO₃). Therefore, the good coulombic efficiency of Na-O₂ cells containing viologen can be explained by the fact that viologen only promotes the formation of NaO₂, and no other degradation products. Formation of Na₂O₂ is not observed, contrary to the case of Li-O₂ batteries, where viologen was shown to promote the 2-electron reduction of O₂ to Li₂O₂.²¹ Loss of rechargeable NaO₂ by its deposition on the separator is not induced by the presence of viologen, which could be attributed to the fact that EtV⁺ facilitates the formation of NaO₂ close to the O₂-

electrolyte interface near the electrode surface, rather than on the separator side.

In conclusion, using redox mediators is an advantageous approach to improve the performance of Na-O₂ cells. On the example of ethyl viologen it is shown that redox mediators can facilitate the solution-based reduction of oxygen to NaO₂, producing higher capacities and higher discharge potentials. The formation of NaO₂ as the main discharge product is confirmed by ex-situ XRD and Raman measurements, while the change in O₂ pressure during cell discharge confirms the stoichiometry of 1e⁻/O₂. UV-vis studies confirm that EtV⁺, rather than EtV⁰, is the active mediator species in the oxygen reduction reaction, thus explaining the high discharge potentials observed. SEM images demonstrate that lower pore clogging is obtained in the presence of ethyl viologen, demonstrating the beneficial effect of introducing a soluble mediator that displaces the reduction of oxygen from the electrode surface to the oxygen-electrolyte interface.

This work has been supported by the "Ministerio de Economía y Competitividad" of Spain (MAT2013-41128-R and MAT2016-78266-P), the "Fondo Europeo de Desarrollo Regional" and the Eusko Jaurlaritza/ Basque Government (project IT-570-13 and ELKARTEK project CICE17). I.L.M. thanks the Universidad del País Vasco (UPV/EHU) for his postdoctoral fellowship. N.G.A. acknowledges EPSRC for an early career fellowship (EP/N024303/1) and support through the Energy SUPERSTORE call "supporting early career researchers" (EP/L019469/1), Royal Society Research Grant (RG130523) and FP7-MC-CIG FunLAB project (630162). There are no conflicts of interest to declare.

References

- (1) Landa-Medrano, I.; Li, C.; Ortiz-Vitoriano, N.; Ruiz de Larramendi, I.; Carrasco, J.; Rojo, T. *J. Phys. Chem. Lett.* **2016**, *7*, 1161–1166.
- (2) Yadegari, H.; Sun, Q.; Sun, X. *Adv. Mater.* **2016**, *28* (33), 7065–7093.
- (3) Bender, C. L.; Schröder, D.; Pinedo, R.; Adelhelm, P.; Janek, J. *Angew. Chem. Int. Ed.* **2016**, *55* (15), 4640.
- (4) Hartmann, P.; Bender, C. L.; Vračar, M.; Dürr, A. K.; Garsuch, A.; Janek, J.; Adelhelm, P. *Nat. Mater.* **2013**, *12* (3), 228–232.
- (5) Xia, C.; Fernandes, R.; Cho, F. H.; Sudhakar, N.; Buonacorsi, B.; Walker, S.; Xu, M.; Baugh, J.; Nazar, L. F. *J. Am. Chem. Soc.* **2016**, *138* (35), 11219–11226.
- (6) Morasch, R.; Kwabi, D. G.; Tulodziecki, M.; Risch, M.; Zhang, S.; Shao-Horn, Y. *ACS Appl. Mater. Interfaces* **2017**, *9* (5), 4374–4381.
- (7) Knudsen, K. B.; Nichols, J. E.; Vegge, T.; Luntz, A. C.; McCloskey, B. D.; Hjelm, J. *J. Phys. Chem. C* **2016**, *120* (20), 10799–10805.
- (8) Aldous, I. M.; Hardwick, L. J. *Angew. Chemie* **2016**, *128* (29), 8394–8397.
- (9) Liu, T.; Kim, G.; Casford, M. T. L.; Grey, C. P. *J. Phys. Chem. Lett.* **2016**, *7*, 4841–4846.
- (10) Landa-Medrano, I.; Sorrentino, A.; Stievano, L.; de Larramendi, I. R.; Pereiro, E.; Lezama, L.; Rojo, T.; Tonti, D. *Nano Energy* **2017**, *37*, 224–231.
- (11) Hartmann, P.; Bender, C. L.; Sann, J.; Dürr, A. K.; Jansen, M.; Janek, J.; Adelhelm, P. *Phys. Chem. Chem. Phys.* **2013**, *15* (28), 11661–11672.
- (12) Hartmann, P.; Heinemann, M.; Bender, C. L.; Graf, K.; Baumann, R.-P.; Adelhelm, P.; Heiliger, C.; Janek, J. *J. Phys. Chem. C* **2015**, *119* (40), 22778–22786.
- (13) Xia, C.; Black, R.; Fernandes, R.; Adams, B.; Nazar, L. F. *Nat. Chem.* **2015**, *7*, 496–501.
- (14) Lutz, L.; Yin, W.; Grimaud, A.; Alves, D.; Corte, D.; Tang, M.; Johnson, L.; Azaceta, E.; Salou-Kanin, V.; Naylor, A. J.; Hamad, S.; Anta, J. A.; Salager, E.; Tena-Zaera, R.; Bruce, P. G.; Tarascon, J. J. *J. Phys. Chem. C* **2016**, *120* (36), 20068–20076.
- (15) Ortiz-Vitoriano, N.; Batcho, T. P.; Kwabi, D. G.; Han, B.; Pour, N.; Yao, K. P. C.; Thompson, C. V.; Shao-Horn, Y. J. *Phys. Chem. Lett.* **2015**, *6*, 2636–2643.
- (16) Bender, C. L.; Hartmann, P.; Vrac, M.; Janek, J. *Adv. Energy Mater.* **2014**, *4* (12), 1301863.
- (17) Yadegari, H.; Li, Y.; Norouzi Banis, M.; Li, X.; Wang, B.; Sun, Q.; Li, R.; Sham, T.-K.; Cui, X.; Sun, X. *Energy Environ. Sci.* **2014**.
- (18) Sun, Q.; Liu, J.; Li, X.; Wang, B.; Yadegari, H.; Lushington, A.; Banis, M. N.; Zhao, Y.; Xiao, W.; Chen, N.; Wang, J.; Sham, T.; Sun, X. *Adv. Funct. Mater.* **2017**.
- (19) He, M.; Lau, K. C.; Ren, X.; Xiao, N.; McCulloch, W. D.; Curtiss, L. A.; Wu, Y. *Angew. Chemie Int. Ed.* **2016**, *128* (49), 15536–15540.
- (20) Abate, I. I.; Thompson, L. E.; Kim, H.; Aetukuti, N. *J. Phys. Chem. Lett.* **2016**.
- (21) Yang, L.; Frith, J. T.; Garcia-Araez, N.; Owen, J. R. *Chem. Commun.* **2015**, *51*, 1705–1708.
- (22) Lacey, M. J.; Frith, J. T.; Owen, J. R. *Electrochem. commun.* **2013**, *26*, 74–76.
- (23) Yin, W.; Yue, J.; Cao, M.; Liu, W.; Ding, J.; Ding, F.; Sang, L.; Fu, Z. *J. Mater. Chem. A Mater. energy Sustain.* **2015**, *3*, 19027–19032.
- (24) Yin, W.; Shadike, Z.; Yang, Y.; Ding, F.; Sang, L. *Chem. Commun.* **2015**, *51*, 2324–2327.
- (25) Pinedo, R.; Weber, D. A.; Bergner, B. J.; Schröder, D.; Adelhelm, P.; Janek, J. *J. Phys. Chem. C* **2016**, *120* (16), 8472–8481.
- (26) McCloskey, B. D.; Garcia, J. M.; Luntz, A. C. *J. Phys. Chem. Lett.* **2014**, *5*, 1230–1235.
- (27) Landa-Medrano, I.; Frith, J. T.; Ruiz de Larramendi, I.; Lozano, I.; Ortiz-Vitoriano, N.; Garcia-Araez, N.; Rojo, T. *J. Power Sources* **2017**, *345*, 237–246.
- (28) Landa-Medrano, I.; Pinedo, R.; Bi, X.; Ruiz de Larramendi, I.; Lezama, L.; Janek, J.; Amine, K.; Lu, J.; Rojo, T. *ACS Appl. Mater. Interfaces* **2016**, *8* (31), 20120–20127.
- (29) Eysel, H. H.; Thym, S. J. *Inorg. Gen. Chem.* **1975**, *411*, 97–192.
- (30) Ma, S.; McKee, W. C.; Wang, J.; Guo, L.; Jansen, M.; Xu, Y.; Peng, Z. *Phys. Chem. Chem. Phys.* **2017**, *19*, 12375–12383.